Scientific Research Publishing

Modeling and Numerical Simulation of Material Science, 2024, 14, 97-106
https://www.scirp.org/journal/mnsms
ISSN Online: 2164-5353
ISSN Print: 2164-5345

SCAPS 1D Simulation of a Lead-Free Perovskite Photovoltaic Solar Cell Using Hematite as Electron Transport Layer

Souleymane Tuo[1*], Konan Boua Marc Kevin Koffi[1], Koffi Arnaud Kamenan[2], Joseph Datte[3], Abé Simon Yapi[4]

[1]Faculty of Sciences and Technologies, University of Man, Man, Côte d'Ivoire
[2]Faculty of Biologicals Sciences, Department of Mathematics, Physics and Chemistry, University of Peleforo Gon Coulibaly, Korhogo, Côte d'Ivoire
[3]Department of Physics, Normal Superior School, Cocody, Côte d'Ivoire
[4]Laboratory of Technologies, University of Felix Houphouet Boigny of Cocody, Abidjan, Côte d'Ivoire
Email: *Souleymane.tuo@univ-man.edu.ci

How to cite this paper: Tuo, S., Koffi, K.B.M.K., Kamenan, K.A., Datte, J. and Yapi, A.S. (2024) SCAPS 1D Simulation of a Lead-Free Perovskite Photovoltaic Solar Cell Using Hematite as Electron Transport Layer. *Modeling and Numerical Simulation of Material Science*, **14**, 97-106.
https://doi.org/10.4236/mnsms.2024.144006

Received: August 26, 2024
Accepted: September 26, 2024
Published: September 29, 2024

Abstract

In recent years, there has been remarkable progress in the performance of metal halide perovskite solar cells. Studies have shown significant interest in lead-free perovskite solar cells (PSCs) due to concerns about the toxicity of lead in lead halide perovskites. $CH_3NH_3SnI_3$ emerges as a viable alternative to $CH_3NH_3PbX_3$. In this work, we studied the effect of various parameters on the performance of lead-free perovskite solar cells using simulation with the SCAPS 1D software. The cell structure consists of α-Fe_2O_3/$CH_3NH_3SnI_3$/PEDOT: PSS. We analyzed parameters such as thickness, doping, and layer concentration. The study revealed that, without considering other optimized parameters, the efficiency of the cell increased from 22% to 35% when the perovskite thickness varied from 100 to 1000 nm. After optimization, solar cell efficiency reaches up to 42%. The optimization parameters are such that, for example, for perovskite: the layer thickness is 700 nm, the doping concentration is 10^{20} and the defect density is 10^{13} cm^{-3}, and for hematite: the thickness is 5 nm, the doping concentration is 10^{22} and the defect concentration is 10^{11} cm^{-3}. These results are encouraging because they highlight the good agreement between perovskite and hematite when used as the active and electron transport layers, respectively. Now, it is still necessary to produce real, viable photovoltaic solar cells with the proposed material layer parameters.

Keywords

$CH_3NH_3SnI_3$, α-Fe_2O_3, SCAPS 1D, Thickness, Doping Defect, Optimisation

1. Introduction

The demand for energy at the global level continues to increase, and one of the direct consequences of this is the depletion of fossil fuels [1]. In addition, their use contributes to the greenhouse effect. Thus causing global warming [2]-[5]. It is, therefore, urgent for States to diversify their "energy mix" by increasing the share of renewable energies, in particular, photovoltaic solar energy, which offers a very promising means of producing electricity because the sun is abundant, free and almost unlimited on the earth [6] [7]. In addition, to make the most of solar energy, photovoltaic technology must address three important factors: efficiency, stability, and low efficiency. Thus, the semiconductors used in the manufacture of these solar cells are the subject of multiple research. So far, silicon is the most commonly used material for the manufacture of photovoltaic cells, accounting for more than 80% of the world's production [4] [8]. Due to its very energy-intensive and expensive production method, other materials now appear to be competitive, in particular, perovskite, which represents a real alternative because of its low cost and thin thickness to create the photovoltaic effect, which makes it possible to produce a large number of solar cells with little material [5] [9]-[12]. The recent implementation of $CH_3NH_3PbX_3$ perovskite absorbers (X = I, Cl, Br) with the organic hole conductor 2,2',7,7'-tetrakis (N, N-di-p-methoxyphenylamine) 9,9'-spirobifluorene (OMETAD spiro) has achieved energy conversion efficiencies (PCE) higher than 23% and has been recognized as an emerging revolution in photovoltaic technologies [13] [14]. However, spiro-OMETAD is costly because its synthesis is more complex and requires rigorous purification steps, which increases production costs [15]. Moreover, lead in perovskite is a limitation due to its potential toxicity and environmental pollution [16]. There are environmental and human health-related complications when lead-based materials are used in perovskite solar cells [13]. So, to solve the problem of lead, we replaced it with tin in perovskite, giving the molecule $CH_3NH_3SnI_3$. Also, in order to use cheaper materials, we opted for PEDOT: PSS as the hole transport layer, replacing the Spiro-Ometad, and hematite (α-Fe_2O_3) instead of TiO_2 [17] [18], which is widely used as an electron transport layer. Hematite is used here for the first time as an electron transport layer. Hematite is the α polymorph of Fe_2O_3. Its gap energy is around 2.1 eV [19] [20]. Moreover, between 600 and 1000 nm, the transparency of α-Fe_2O_3 thin films varies between 70% and 85%, giving them transparency in the visible range [21]. Moreover, hematite is widely available and inexpensive to produce. Hematite could ensure the efficient transfer of electrons generated by light absorption to the electrode, thus contributing to the production of electric current in solar cells.

Before implementing physical devices experimentally, it is often necessary to use simulation to establish orders of magnitude for the device parameters. Numerical simulation is a powerful tool for understanding and describing a physical device. Photovoltaic solar cells are governed by the properties of semiconductors. So, it is possible to understand the parameters that limit or improve the performance of

photovoltaic solar cells through simulation, as mentioned by [8]. In this study, we used SCAPS to simulate photovoltaic solar cells with a view to optimizing them [22]-[24].

The main objective of this study is to highlight the effect of several physical parameters on the photovoltaic performance of the solar cell based on the perovskite $CH_3NH_3SnI_3$ as an absorbent layer with the SCAPS 1D simulation tool. Particular attention will be paid to the study of the effect of the thickness, defect density and doping concentration of each layer of the cell on the characteristics of the solar cell in order to predict the optimal parameters for obtaining high electrical conversion efficiency.

2. Device Modelling Parameters

The α-Fe_2O_3/$CH_3NH_3SnI_3$/PEDOT: PSS structure studied is a planar structure given in **Figure 1(a)**. Therefore, it is composed of a hematite (α-Fe_2O_3) layer of type n, used as an electron transport material (ETL) and at the same time as a front contact (anode), hybrid halogenated perovskite ($CH_3NH_3SnI_3$) of type p which was used as an absorbent material and PEDOT: PSS as a hole transport material (HTL). The energy band alignment is shown in **Figure 1(b)**. The conduction band offset at α-Fe_2O_3/ $CH_3NH_3SnI_3$ interface is +0.27 eV, which is crucial for the migration of generated photoelectrons to the front contact. A similar study is carried out by [25], where the PCBM is the electron transport layer. **Table 1** summarises the simulation parameters for the configuration. The given parameters *Eg* is the energy bandgap, ε_r is the relative permittivity, χ being the electron affinity, μ_n and μ_p are the electron and hole mobilities, N_t is the defect density, respectively. *Na* and *Nd* are the densities of acceptor and donor materials, whereas *Nc* and *Nv* are the effective densities of the conduction band and valence band. The parameter values not included in the table are set identically for all layers. Neutral Gaussian distribution defect is adopted with characteristic energy being set to 0.1 eV [26]. The hole capture cross section is set to 1×10^{-15} cm^2, with the thermal velocity of all carriers is fixed at 10^7 cm/s [27]. No optical reflectance is considered in the simulation and we have optimized the numerical parameters used in the study using the control variable method.

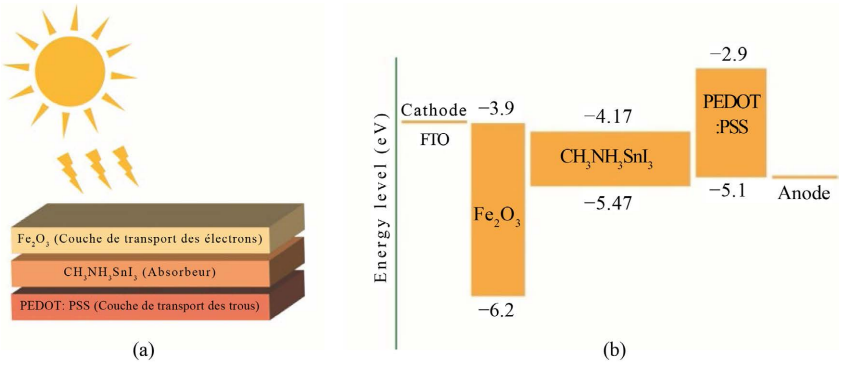

Figure 1. Simulated solar cell: (a) configuration of the cell; (b) energy band alignment.

After performing simulations in SCAPS using the parameters in Table 1, we obtained the solar cell output parameters: Short circuit current density (Jsc), Open circuit Voltage (Voc), Fill factor (FF), and Power conversion efficiency (PCE).

Table 1. Simulation parameters for solar cell material layers.

Materials	$CH_3NH_3SnI_3$ [10]-[12]	PEDOT: PSS [12]	α-Fe_2O [19] [20]
E_g (ev)	1.3	2.2	2.3
X (ev)	4.170	2.900	3.900
$\varepsilon/\varepsilon_0$	8.200	3.000	9.800
Nc (cm^{-3})	1×10^{18}	1×10^{15}	3×10^{18}
Nv (cm^{-3})	1×10^{18}	1×10^{18}	1×10^{19}
μ_e (cm^{-2}/Vs)	2000	1×10^{-1}	2×10^{-3}
μ_h (cm^{-2}/Vs)	300	2×10^{-3}	5×10^{-5}
N_d (cm^{-3})	-	-	4.003×10^{20}
N_a (cm^{-3})	5×10^{14}	1×10^{18}	-
σ_p (cm^{-2})	8.200	3.000	9.800
N_t (cm^{-3})	1.019E+13	1.042E+13	1.042E+13

3. Results and Discussions

3.1. Effect of Thickness of Absorber Layer $CH_3NH_3SnI_3$

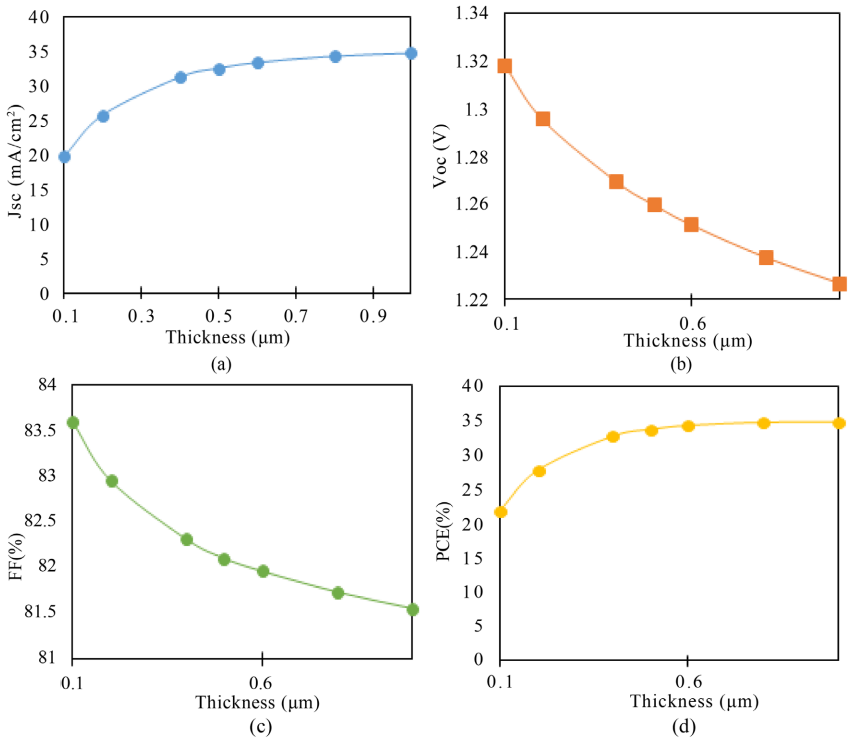

Figure 2. Variation of solar cell parameters with thickness of $CH_3NH_3SnI_3$: (a) Jsc; (b) Voc; (c) FF; (d) PCE.

The thickness of the absorbent layer plays a very important role in the performance of the cell. Thus, to highlight this, we varied the thickness from 100 nm to 1000 nm. The simulation results are shown in **Figure 2**.

It can be seen that when the thickness of the absorbent layer (perovskite) is varied, the current density Jsc increases. This is because more photons are captured in the volume of the material. Indeed, when the number of absorbed photons increases in the volume of the material, there is an increase in the electron-hole pairs generated and consequently, the current also increases, hence, the increase in conversion efficiency. Thus, the Power Conversion Efficiency (PCE) can reach 34.54% at 700 nm. A slight decrease in Voc with thickness is due to the increased rate of recombination. The decrease in form factor with increasing absorber thickness can be attributed to increasing the series resistance of the absorber, as proved by [28] [29].

3.2. Effect of Doping Concentration of Absorber Layer

Doping is a very important process used to improve the properties of semiconductor devices, such as solar cells [30]. Doping of a photoactive material in the solar cell architecture decides the electrical behavior of the layers, which will affect the performance of the device [13]. For this study, the thickness of the perovskite layer is fixed at 700 nm, and the thickness of the hematite (the ETL layer) and PEDOT: PSS (the HTL layer) are fixed at 5 nm. We varied the perovskite doping from 1.10^{10} cm^{-3} to 1.10^{22} cm^{-3}.

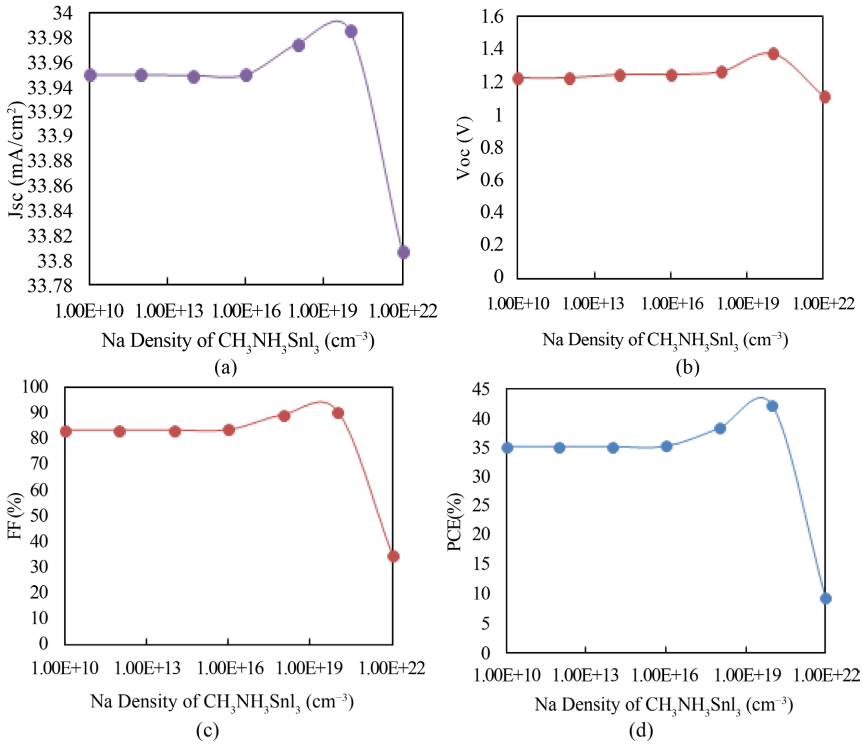

Figure 3. Variation of solar cell parameters with doping of CH3NH3SnI3: (a) Jsc; (b) Voc; (c) FF; (d) PCE.

Figure 3 above shows that when 1E+10 cm^{-3} ≤ Na < 1E+16 cm^{-3}, the doping concentration of the absorber has no influence on the photovoltaic parameters of the cell. But, we can observe that from 1E+16 cm^{-3} to 1E+20 cm^{-3}, the increase in absorber doping concentration leads to an improvement in solar cell parameters. This is due to a reduction in the potential barrier and, therefore, a reduction in the space charge region. Above 1E+20 cm^{-3}, the solar cell parameters drop in value, especially on short-circuit current and efficiency, because of the decrease in the collection of generated photo carriers. This is possible due to the increased recombination rate of charge carriers inside the perovskite absorbing layer. So, the concentration of 10^{20} cm^{-3} represents the optimal value to achieve the maximum performance of our solar cell.

3.3. Effect of Defect Density Absorber Layer

Defects are inevitable in the absorbent layer; they can exist in the volume and on the surface. Point defects such as gaps, interstitial defects, Schottky and Frenkel [31]. We considered a neutral Gaussian distribution defect with 0.1 eV characteristic energy in the volume, as did Nithya K.S. and Sudheer K.S. in their study [26]. The defect density varies from 10^{13} to 10^{16} cm^{-3} in the absorbent layer ($CH_3NH_3SnI_3$).

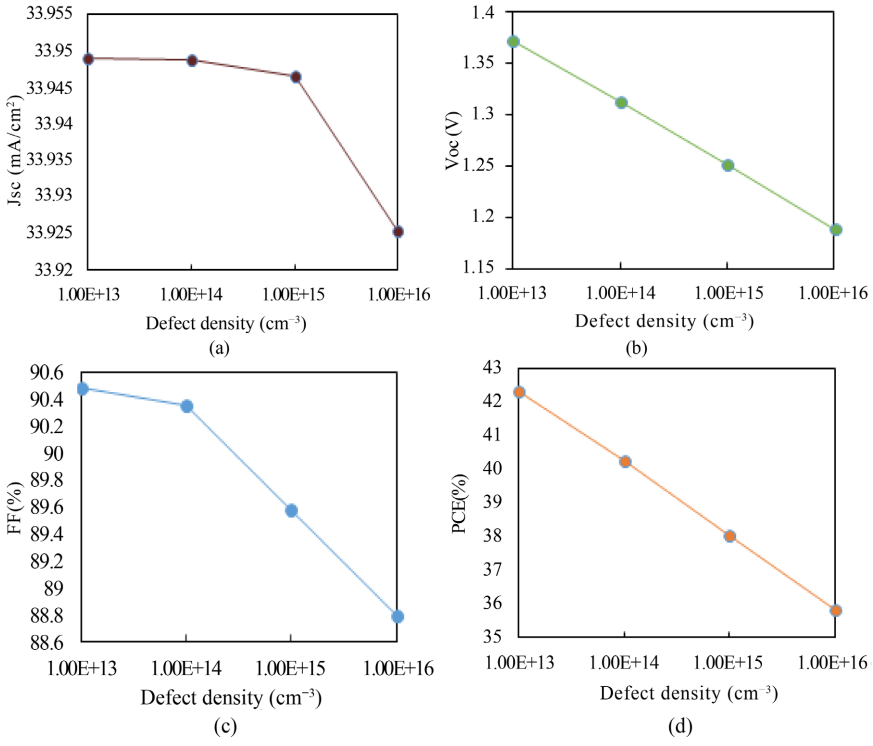

Figure 4. Variation of solar cell parameters with defect density Nt (cm^{-3}): (a) Jsc; (b) Voc; (c) FF; (d) PCE.

As expected, the high defect densities in the absorbing layer material limit the performance characteristics of the solar cell, as related by [11] [26] [32]-[34]. According to the results of our simulation, all solar cell parameters are significantly

reduced when the defect concentration of the absorbing layer increases. This is because these defects introduce deep or shallow levels into the energy bandgap. Because of these defects, charge carriers can become trapped and facilitate non-radiative electron-hole recombination [35]. (**Figure 4**)

Thus, in this study, to optimize the solar cell, it is advisable to retain a defect density of the order of 10^{13} cm^{-3} for the absorbent layer ($CH_3NH_3SnI_3$).

4. Conclusions

The SCAPS 1D software allowed us to simulate the photoelectric behavior of the perovskite-based solar cell with structure α-Fe_2O_3/ $CH_3NH_3SnI_3$/PEDOT: PSS. The photovoltaic solar cell is characterized by its J(V) curve. The parameters of the simulation relate to the thickness, the density of the defects and the doping concentration of the absorbent layer. The best performance of the cell is achieved for: Jsc = 33.948884 mA/cm^2, Voc = 1.3724 V, FF = 90.80% and PCE = 42.3%, when the Perovskite absorbent layer has 700 nm thickness, doped with a Na acceptor concentration of 10^{20} cm^{-3}; beyond this concentration, the cell yield drops.

In perspective, in order to verify these encouraging results, an experimental study should be carried out to understand the limits of the real solar cell.

Acknowledgements

The authors sincerely thank Dr. Marc Burgelmann and his team at the University of Gent, Belgium, for providing the scientific community with this simulation program.

Conflicts of Interest

The authors declare no conflicts of interest regarding the publication of this paper.

References

[1] Wang, J. and Azam, W. (2024) Natural Resource Scarcity, Fossil Fuel Energy Consumption, and Total Greenhouse Gas Emissions in Top Emitting Countries. *Geoscience Frontiers*, **15**, Article 101757. https://doi.org/10.1016/j.gsf.2023.101757

[2] Kanna, V.I., Roseline, S., Balamurugan, K., Jeeva, S. and Augastin Santhiyagu, I. (2024) The Effects of Greenhouse Gas Emissions on Global Warming. In: Rahimpour, M.R., Ed., *Encyclopedia of Renewable Energy, Sustainability and the Environment*, Elsevier, 143-154. https://doi.org/10.1016/b978-0-323-93940-9.00216-4

[3] Kocak, E., Ulug, E.E. and Oralhan, B. (2023) The Impact of Electricity from Renewable and Non-Renewable Sources on Energy Poverty and Greenhouse Gas Emissions (GHGs): Empirical Evidence and Policy Implications. *Energy*, **272**, Article 127125. https://doi.org/10.1016/j.energy.2023.127125

[4] Khan, A.A., Reichel, C., Molina, P., Friedrich, L., Subasi, D.M., Neuhaus, H., *et al.* (2024) Global Warming Potential of Photovoltaics with State-of-the Art Silicon Solar Cells: Influence of Electricity Mix, Installation Location and Lifetime. *Solar Energy Materials and Solar Cells*, **269**, Article 112724. https://doi.org/10.1016/j.solmat.2024.112724

[5] Babayigit, A., Boyen, H. and Conings, B. (2018) Environment versus Sustainable

Energy: The Case of Lead Halide Perovskite-Based Solar Cells. *MRS Energy & Sustainability*, **5**, Article No. 15. https://doi.org/10.1557/mre.2017.17

[6] Qiu, Z. and Li, P. (2019) Solar Energy Resource and Its Global Distribution. In: Zhao, X. and Ma, X., Eds., *Advanced Energy Efficiency Technologies for Solar Heating, Cooling and Power Generation*, Springer International Publishing, 1-30. https://doi.org/10.1007/978-3-030-17283-1_1

[7] Goel, M., Verma, V.S. and Tripathi, N.G. (2022) Sun: Unlimited Energy Resource on Earth. In: Goel, M., Verma, V.S. and Tripathi, N.G., Eds., *Solar Energy*, Springer, 15-26. https://doi.org/10.1007/978-981-19-2099-8_2

[8] Hajji, M., Ajili, M., Charrada, G., Jebbari, N., Garcia-Loureiro, A. and Turki Kamoun, N. (2024) Comprehensive Study on the Physical Properties of CuO-ZnO Thin Films: Insights into Solar Cell Simulation. *Optical Materials*, **155**, Article 115887. https://doi.org/10.1016/j.optmat.2024.115887

[9] Ghahremanirad, E., Olyaee, S., Nejand, B.A., Nazari, P., Ahmadi, V. and Abedi, K. (2018) Improving the Performance of Perovskite Solar Cells Using Kesterite Mesostructure and Plasmonic Network. *Solar Energy*, **169**, 498-504. https://doi.org/10.1016/j.solener.2018.05.012

[10] Ngulezhu, T., Abdulkarim, A.S., Rawat, S., Singh, R.C., Singh, P.K., Singh, D., *et al*. (2024) Stable Lead Free Perovskite Solar Cells Based on Bismuth Doped Perovskite Materials. *Chemical Physics Impact*, **9**, Article 100689. https://doi.org/10.1016/j.chphi.2024.100689

[11] Oyedele, S.O., Soucase, B.M. and Aka, B. (2016) Numerical Simulation and Performance Optimization of Cu(In, Ga)Se_2 Solar Cells. *IOSR Journal of Applied Physics*, **8**, 1-11. https://doi.org/10.9790/4861-0804040111

[12] Li, M., Zhou, J., Tan, L., Li, H., Liu, Y., Jiang, C., *et al*. (2022) Multifunctional Succinate Additive for Flexible Perovskite Solar Cells with More than 23% Power-Conversion Efficiency. *The Innovation*, **3**, Article 100310. https://doi.org/10.1016/j.xinn.2022.100310

[13] Coulibaly, A.B., Oyedele, S.O., Kre, N.R. and Aka, B. (2019) Comparative Study of Lead-Free Perovskite Solar Cells Using Different Hole Transporter Materials. *Modeling and Numerical Simulation of Material Science*, **9**, 97-107. https://doi.org/10.4236/mnsms.2019.94006

[14] Li, S., Cao, Y., Li, W. and Bo, Z. (2021) A Brief Review of Hole Transporting Materials Commonly Used in Perovskite Solar Cells. *Rare Metals*, **40**, 2712-2729. https://doi.org/10.1007/s12598-020-01691-z

[15] Abdellah, I.M., Chowdhury, T.H., Lee, J., Islam, A., Nazeeruddin, M.K., Gräetzel, M., *et al*. (2021) Facile and Low-Cost Synthesis of a Novel Dopant-Free Hole Transporting Material that Rivals Spiro-OMeTAD for High Efficiency Perovskite Solar Cells. *Sustainable Energy & Fuels*, **5**, 199-211. https://doi.org/10.1039/d0se01323d

[16] Raj, K. and Das, A.P. (2023) Lead Pollution: Impact on Environment and Human Health and Approach for a Sustainable Solution. *Environmental Chemistry and Ecotoxicology*, **5**, 79-85. https://doi.org/10.1016/j.enceco.2023.02.001

[17] Fatima, Q., Haidry, A.A., Zhang, H., El Jery, A. and Aldrdery, M. (2024) A Critical Review on Advancement and Challenges in Using TiO_2 as Electron Transport Layer for Perovskite Solar Cell. *Materials Today Sustainability*, **27**, Article 100857. https://doi.org/10.1016/j.mtsust.2024.100857

[18] Wu, J. and Huang, Q. (2022) Properties of TiO_2 Film Prepared by Anodization as Electron Transport Layer for Perovskite Solar Cells. *International Journal of Electrochemical Science*, **17**, Article 220223. https://doi.org/10.20964/2022.02.26

[19] Cai, J., Tang, X., Zhong, S., Li, Y., Wang, Y., Liao, Z., *et al*. (2023) Elucidation the Role of Co-MOF on Hematite for Boosting the Photoelectrochemical Performance toward Water Oxidation. *International Journal of Hydrogen Energy*, **48**, 12342-12353. https://doi.org/10.1016/j.ijhydene.2022.12.165

[20] Gartner, M., Crisan, M., Jitianu, A., Scurtu, R., Gavrila, R., Oprea, I., *et al*. (2003) Spectroellipsometric Characterization of Multilayer Sol-Gel Fe_2O_3 Films. *Journal of Sol-Gel Science and Technology*, **26**, 745-748. https://doi.org/10.1023/a:1020706423230

[21] Waychunas, G.A., Kim, C.S. and Banfield, J.F. (2005) Nanoparticulate Iron Oxide Minerals in Soils and Sediments: Unique Properties and Contaminant Scavenging Mechanisms. *Journal of Nanoparticle Research*, **7**, 409-433. https://doi.org/10.1007/s11051-005-6931-x

[22] Burgelman, M., Nollet, P. and Degrave, S. (2000) Modelling Polycrystalline Semiconductor Solar Cells. *Thin Solid Films*, **361**, 527-532. https://doi.org/10.1016/s0040-6090(99)00825-1

[23] Valeti, N.J., Prakash, K. and Singha, M.K. (2023) Numerical Simulation and Optimization of Lead Free $CH_3NH_3SNI_3$ Perovskite Solar Cell with $CuSbS_2$ as HTL Using SCAPS 1D. *Results in Optics*, **12**, Article 100440. https://doi.org/10.1016/j.rio.2023.100440

[24] Vaish, S. and Kumar Dixit, S. (2023) Study the Effect of Total Defect Density Variation in Absorbing Layer on the Power Conversion Efficiency of Lead Halide Perovskite Solar Cell Using SCAPS-1D Simulation Tool. *Materials Today*: *Proceedings*, **91**, 17-20. https://doi.org/10.1016/j.matpr.2023.05.374

[25] Mandadapu, U. (2017) Simulation and Analysis of Lead Based Perovskite Solar Cell Using SCAPS-1D. *Indian Journal of Science and Technology*, **10**, 1-8. https://doi.org/10.17485/ijst/2017/v11i10/110721

[26] Nithya, K.S. and Sudheer, K.S. (2020) Numerical Modelling of Non-Fullerene Organic Solar Cell with High Dielectric Constant ITIC-OE Acceptor. *Journal of Physics Communications*, **4**, Article 025012. https://doi.org/10.1088/2399-6528/ab772a

[27] Oliver, R.D.J., Caprioglio, P., Peña-Camargo, F., *et al*. (2021) Understanding and Suppressing Nonradiative Losses in Methylammonium-Free Wide Bandgap Perovskite Solar Cells. *Energy & Environmental Science*, **15**, 714-726. https://doi.org/10.1039/D1EE02650J

[28] Lazemi, M., Asgharizadeh, S. and Bellucci, S. (2018) A Computational Approach to Interface Engineering of Lead-Free $CH_3NH_3SnI_3$ Highly-Efficient Perovskite Solar Cells. *Physical Chemistry Chemical Physics*, **20**, 25683-25692. https://doi.org/10.1039/c8cp03660h

[29] Hervé, J., Tchognia, N., Hartiti, B., Ndjaka, J.-M. and Ridah, A. (2015) Performances des cellules solaires à base de Cu_2ZnSnS_4 (CZTS): Une analyse par simulations numériques via le simulateur SCAPS. *Afrique Sciences*, **11**, 16-23.

[30] Pramanik, M.B., Al Rakib, M.A., Siddik, M.A. and Bhuiyan, S. (2024) Doping Effects and Relationship between Energy Band Gaps, Impact of Ionization Coefficient and Light Absorption Coefficient in Semiconductors. *European Journal of Engineering and Technology Research*, **9**, 10-15. https://doi.org/10.24018/ejeng.2024.9.1.3118

[31] Saikia, D., Das, C., Chetia, A., Betal, A. and Sahu, S. (2024) Numerical Simulation of All Inorganic $CsPbiBr_2$ Perovskite Solar Cells with Diverse Charge Transport Layers Using DFT and SCAPS-1D Frameworks. *Physica Scripta*, **99**, Article 095946. https://doi.org/10.1088/1402-4896/ad6aa8

[32] Soro, D., Sylla, A., Gbané, A., Franck, B., Guaita, J., Bouich, A., Toure, S. and Marí, B.

(2024) Modeling and Simulation of an Organic Photovoltaic Cell: ITO/MoO_3/CAR-APA/PCBM/Alq_3/Al with SCAPS. *Modeling and Numerical Simulation of Material Science*, **14**, 79-96. https://doi.org/10.4236/mnsms.2024.143005

[33] Ashok, A., Cano, F.J., Reyes-Vallejo, O., Hernández-Rodríguez, Y.M., Cigarroa-Mayorga, O.E., Vega-Pérez, J., *et al*. (2023) SCAPS Simulation on CIGSe Thin Film Solar Cells: Effect of the Defects. 2023 20*th International Conference on Electrical Engineering, Computing Science and Automatic Control* (*CCE*), Mexico City, 25-27 October 2023, 1-6. https://doi.org/10.1109/cce60043.2023.10332898

[34] Touafek, N. and Mahamdi, R. (2014) Excess Defects at the CdS/CIGS Interface Solar Cells. *Chalcogenide Letters*, **11**, 589-596.

[35] Lee, Y.M., Maeng, I., Park, J., Song, M., Yun, J., Jung, M., *et al*. (2018) Comprehensive Understanding and Controlling the Defect Structures: An Effective Approach for Organic-Inorganic Hybrid Perovskite-Based Solar-Cell Application. *Frontiers in Energy Research*, **6**, Article 128. https://doi.org/10.3389/fenrg.2018.00128